Available online at www.sciencedirect.com
ScienceDirect
Current Opinion in Solid State and Materials Science 10 (2006) 217–229
Current Opinion in Solid State & Materials Science

Optical properties of oxide glasses containing transition metals: Case of titanium- and chromium-containing glasses

Manal Abdel-Baki [a,*], Fouad El-Diasty [b]

[a] National Research Center, Glass Department, Dokki, Giza, Egypt
[b] Physics Department, Faculty of Science, Ain Shams University, Cairo 11566, Egypt

Received 2 August 2007; accepted 6 August 2007

Abstract

One of the major driving forces for the development of new glasses is the demand for high optical non-linearity with reduced cost and a higher damage resistance. Oxide glasses with large non-linear refractive index and non-linear absorption coefficient are promising materials for fiber telecommunication and for non-linear optical devices such as ultrafast optical switches, power limiters, real time holography, self-focusing, white-light continuum generation and photonic applications. To get insight into the optical absorption in amorphous materials, studies are still needed for revealing the nature of photoelectronic excitations in these materials by comparison with that in crystals which have been understood firmly based on band theory. Although the IR absorption loss in oxide glasses is larger than of fluorides, low light scattering loss is expected in these oxide glasses because they have lower glass transition temperature. In addition, small concentration of dopant such as alkaline metal and alkaline earth metal elements gives rise to the structural relaxation of the frozen-in density fluctuations even below glass transition temperature T_g, adding to the reduction of T_g as well. A review of the fundamentals and recent research advances in optical properties of oxide glasses containing chromium or titanium is presented.

Keywords: Oxide glasses; Optical properties; Chromium; Titanium; Transition metals

1. Introduction

Glasses are important optical materials usually are made to be transparent in the visible spectrum. Since glasses are amorphous materials, therefore, they do not exhibit optical anisotropy that is characteristic of some crystals. Thus, the structure of the typical glass of binary oxide formers B_2O_3, SiO_2, GeO_2, and P_2O_5 is accounted in terms of three-dimensional infinite cross-linking of units forming short-range order with no long-range order. Most types of glasses are made by fusion of formers with other modifier oxides. An important difference between crystalline and amorphous materials involves the effect of composition changes. Glasses are generally absorbing light energy in the ultraviolet due to the electronic transitions in interior molecules, and in the infrared region due to molecular vibrations.

2. Oxide glasses

The increased glass-formation tendency of oxides is a result of fundamental features of the chemical bond. Starting from the left-hand side of the periodic table, owing to the high difference of the electronegativity, highly connective ionic lattices of oxide exist, yielding packing of units with a high density. Going on to the right-hand side, an increased contribution of covalent bonding occurs, and at the same time the coordination number decreases. Especially in the upper series, the bonds are more direct to the oxygen ligands. Due to the ability to form 2-fold covalent bonds, oxygen is specially suited to link structural units having coordination numbers of 3, 4, or 6. It makes

* Corresponding author. Tel.: +20 2 22879706.
E-mail address: manalbaki@yahoo.com (M. Abdel-Baki).

1359-0286/$ - see front matter © 2007 Elsevier Ltd. All rights reserved.
doi:10.1016/j.cossms.2007.08.001

possible continuous cross-linking leading to highly polymeric network structure.

Glasses result from many possible combinations of network-forming oxides together with one or several modifier alkali oxides RO (R = Li, Na, or K). As the alkali oxide is added to glass, the optical density in the ultraviolet at wavelength longer than the absorption edge is directly proportional to the alkali concentration. The intensity of absorption increased in the order of lithium, sodium, and potassium for a given alkali concentration. Incorporating the so-called intermediate oxides, Al_2O_3, Fe_2O_3, TiO_2, ZrO_2, etc., into the glasses leads to an enormous extension of possible vitreous materials (structural configuration possibilities) with special physical properties. Often it has a maximum in the region of the eutectic composition, which can be interpreted as a compositional region of inhibited crystallization due to disorder. The incorporation of network modifiers alters fundamentally the glass properties. Hence, the molar volume will decrease and the glass transition temperature is lowered due to the reduced degree of cross-linking.

The requirements of electroneutrality, allowing at most little charge separation, suggest the formation of triangular units of $BO_{3/2}$ or of tetrahedral units such as $[BO_{4/2}]^-$, $SiO_{4/2}$, $GeO_{4/2}$, and $[PO_{4/2}]^-$. Zachariasen [1], the founder of the theory of glass structure, defined these units to be the origin of a molecular-like short-range order.

According to Goldschmidt [2], the formation of the glass needs the ionic radius ratio of the cation, R, to the oxygen ion lies in the range of 0.2–0.4. Since the radius ratio in this range facilitates cations surrounded by four oxygen ions in the form of tetrahedral. So the glass network consists of tetrahedral units connected at all four corners, just as in the corresponding crystals, but with no periodic and symmetric arrangement. Therefore, the glass network extends in three dimensions where the average behavior is the same in all directions giving an isotropic character for the glass.

Stanworth [3] classified oxides into three groups according to the electronegativity of the cation. Since the oxygen is the anion, the fractional ionic character of the cation–anion bond could be used to scale out the different groups. Cations which have high electronegativity and form with the oxygen a fractional ionic character near 50% should act as network formers (group 1) and produce good glasses. In the second group, the cations are known as intermediate since they have intermediate electronegativities. In this case, the cations form slightly more ionic bonds with oxygen and can not form glasses by themselves, but can partially replace cations from the first group. In the third group cations have very low electronegativities, and therefore, they form highly ionic bonds with oxygen and obviously they never act as network formers. These cations are termed modifiers since they serve only to modify the network structure created by network-forming oxides.

If a modifier oxide such as NaO_2 is added to silica glass, the bond in the network is broken and the relatively mobile sodium ion becomes a part of the structure. Zachariasen [1] and Warren and Biscoe [4] suggested, as shown in Fig. 1, that the network formers form some type of network, with bridging (BO) and non-bridging oxygen bonds (NBO's). The relative abundance of NBO as negatively charged terminal oxygen atoms is important in determining the optical, thermodynamic and dynamic properties of glasses [5,6]. It can be seen from the figure that for SiO_2 the bond angle at the bridging oxygen atom is less 180°. Variation of such angles around an average value of 150° and the freedom of rotation about the Si–O bonds make possible the occurrence of a broad distribution of structural configurations, yielding a continuous random network structure with no, or strongly reduced, long-range order. An increase of the polarizability arises from the negative charged non-bridging atoms, and thus the anharmonicity of thermal vibrations also increases. Consequently, the coefficient of thermal expansions will increase. The higher the content of network modifier in the glass, the higher is the concentration of non-bridging atoms.

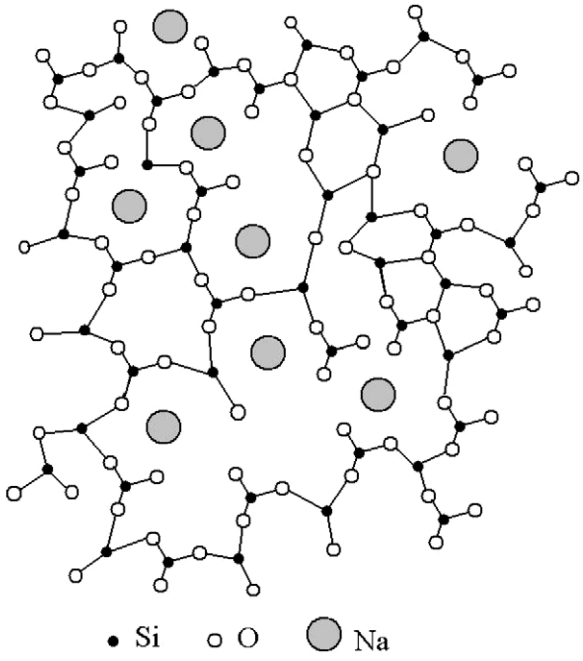

Fig. 1. Schematic representation of random network model of alkali silicate glasses. Silicon is shown 3-coordinated for clarity.

Therefore, the essential structural prerequisite for a preference of glass formation is the existence of units with coordination number of 2, 3, or 4, which are connected by a divalent linking atom, e.g., oxygen.

3. Optical properties of oxide glasses

There are many advanced and exciting applications of glasses in optics: optical fibers as waveguides for long and fast telecommunications, laser hosts, and optical components for medical and outer space studies. Other modern glasses are glasses that change absorption with light level

(photochromic) and electric field (electrochromic), glasses for gradient index lenses, new glasses such as fluorides with different optical properties for silicate planar waveguides, sensors, and chalcogenide glasses with high non-linear optical properties for switching, all-optic devices and photonic applications.

The linear refractive index, n, and its dispersive wavelength dependence are important parameters that determine the suitability of oxide glasses as optical materials. The propagation of electromagnetic waves dependences on the optical constants of materials n and k (the extinction coefficient), where n affects the phase of light waves propagate in the material while k affects its amplitude. Fused silica glass for instant is used extensively in the fiber optics industry because the absorption and scattering losses are so small that light can travel many kilometers down the fiber before being fully attenuated. The presence of chemical additives can alter the refractive index and the transmission range. Glasses are differ considerably in structure and thus in the position and intensity distribution of their electronic absorption and vibrational spectra. Color glass filters are made by adding semiconductors with the band gaps in the visible spectral region during the fusion process.

For practical purposes, the mean dispersion is the difference in refractive indices of two wavelengths, $\Delta n = n_1 - n_2$. In the visible spectral region, it is also referred to as the main dispersion, defined as $n_F - n_C$, in terms of refractive indices for certain spectral lines of cadmium, such as F = 479.99 nm for n_1 and C = 643.85 nm for n_2. The quantity $(n_F - n_C)/(n_d - 1)$, where n_d is the index at the green line 546.07 nm of the mercury spectrum, is known as the relative dispersion. The reciprocal of the relative dispersion is defined as the Abbe number, υ. Highly refractive glasses tend to have smaller Abbe numbers, i.e., high relative dispersion. A high refractive index is desirable to increase glass reflectivity (shiny appearance).

The portions of the dispersion curve in-between the anomalous-dispersion branches (the normal-dispersion parts) are known to represent a normal dispersion obeying, as good approximation, the empirical Cauchy dispersion equation

$$n = A + \frac{B}{\lambda^2} \tag{1}$$

where A and B are known as Cauchy coefficients which are characteristic of the material.

The factors affecting refractive-index of the glass are [7]:

1. Polarizability of the first neighbor ions coordinated with it (anion).
2. Field intensity Z/a^2 (i.e., polarization power), where Z is the valence of the ion (ionic charge) and a is the distance of separation (ionic radius).
3. Coordination number of the ion.
4. Non-bridging oxygen bonds (NBO's).
5. Electronic polarizability of the oxide ion.
6. Optical basicity of the glasses.

According to Fajan's rules [8] the first two factors mean that to increase electronic polarizability of the material a small positive ion (cation), a large negative ion (anion), and large charges on either ion are required. In the scope of previous factors, the refractive indices behavior of the different glass samples can be analyzed and explained.

4. Optical basicity

The chemical interactions between the glass components are of acid–base character. The oxygen atoms in glasses behave as Lewis' bases and they can transfer part of their negative charge to the cations. The ability of oxygen to transfer the negative charges is the greatest when it is situated in the surroundings of weak cations, such as the alkalis. Duffy and coworkers [9,10] proposed the concept of optical basicity based on the experimental shift of the ultraviolet spectrum of a probe incorporated in various oxides. Duffy proposed a parameter Λ that permits a comparison of the acid–base character of oxides.

The optical basicity Λ, of an oxidic medium, is the average electron donor power of all the oxide atoms comprising the medium. Increasing basicity results in increasing negative charge on the oxygen atoms and, thus, increasing covalency in the cation-oxygen bonding. The optical basicity could be predicted from the glass compositions and from the basicity moderating parameters of the various cations present.

5. Nonlinear optical properties of glasses

Strong electric field E or intense radiation fields can alter the optical properties of the materials and the polarization P of the material is given by [11]:

$$P = \chi^{(1)}E + \chi^{(2)}EE + \chi^{(3)}EEE \tag{2}$$

where $\chi^{(1)}$, $\chi^{(2)}$, and $\chi^{(3)}$ are the first-, second-, and third-order susceptibilities. The first-order susceptibility is response for the linear optical properties such as reflection, refraction, absorption, and scattering. The second-order susceptibility applies only to materials without inversion symmetry such as birefringent crystals and poled glasses. It leads to phenomena such as second harmonic and difference frequency generation, optical parametric oscillation, the linear electro-optic (Pockel's) effect, and the photorefractive effect. Two-photon absorption (TPA), self focusing due to alteration of the second-order refractive index n_2 (intensity-dependent refractive index) and the quadratic Kerr effect all arise due to third-order susceptibility. It also leads to third harmonic generation and stimulated Raman and Brillouin scattering.

The optical properties of multi-component oxide glasses are determined by the concentration of the transition metal cations (i.e., bond polarizability) rather than by the number of non-bridging oxygen [12]. The microscopic non-linear properties of the glasses are determined by n_2 and the third-order non-linear optical susceptibility, χ^3 (in units

of m^2/V^2). Here n_2 denotes the non-linear optic coefficient or the second-order index of refraction (in units of m^2/W). It gives the rate at which the refractive index increases with increasing optical intensity. The optical Kerr Effect leads to an intensity-dependent non-linear refractive index [13],

$$n = n_o + n_2 I \tag{3}$$

where I is the light intensity and n_o represents the weak-field refractive index. The second-order index of refraction, n_2, is required for soliton propagation in the optical telecommunication fibers and also used in all optical switching schemes. A major concern for high power lasers is to minimize this non-linearity so as to prevent catastrophic self-focusing and beam breakup. In contrast, for all-optical switching glass devices a large n_2 value and a rapid response time are needed to minimize the optical power requirements. In many of the glassy oxides that have low to moderate refractive indices (i.e., $n < 1.7$), the bond polarizability and hyper-polarizability, and therefore the linear and non-linear refractive indices, are dominated by the Oxygen, O anion. Boling et al. [14] derived a semi-empirical relation for predicting the second-order index of refraction, n_2, for glasses from the linear refractive index, n_d, which is given by:

$$n_2(10^{-13}\ \text{esu}) = K\frac{n_d - 1}{v^{5/4}} \tag{4}$$

where K is an empirical constant.

According to the Boling's semi-empirical equation, the third-order non-linear optical susceptibility, χ^3, of the material is strongly dependent on the second-order index of refraction, n_2, and linear refractive index. According to Vogel et al. [12], χ^3 is given by the following relation:

$$\chi^3 = \frac{n_d}{12\pi} n_2 \tag{5}$$

6. Optical properties in terms of electron band structure

In Fig. 2, classification of the principal types of electron transitions in materials is shown and they are:

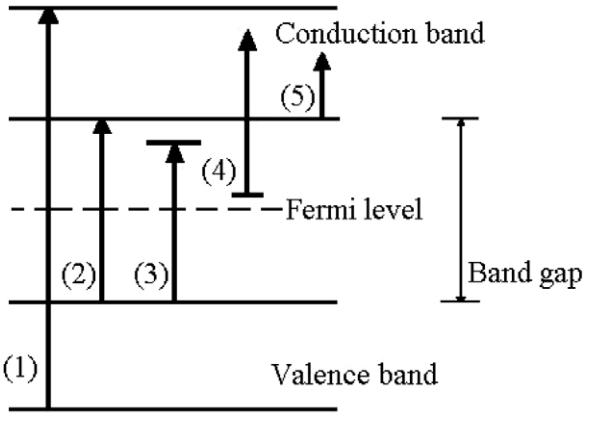

Fig. 2. Schematic diagram for the different optical absorption mechanisms in materials.

1. High energy interband transitions.
2. Transitions across the band gap-absorption edge.
3. Exciton generation (bound electron-hole pair).
4. Impurity level excitation.
5. Intraband transition.

However, in case of interband transitions different mechanisms are available. The highest energy transitions are those from the bottom of the valance band to the top of conduction band giving rise to a frequency dependence of the attenuation coefficient, α. Transition from the top of the valance band to the bottom of the conduction band also occurs. The absorption edge occurs at $h\nu = E_g$, the gap energy.

On the other hand, α decreases rapidly once the energy drops below the band gap energy E_g. Since there is no energy states for the electros to by occupied, so they cannot absorb the energy of incident photons. With exciton generation a bounded electron-hole pair is produced. The electron is trapped in a localized energy level in the band gap while the hole remains mobile in the valance band.

Exciton can dissociate into independent free carriers or can recombine with the emission of a photon or phonon. Other lower energy transition (less than E_g) is the excitation of electrons from localized trap sites in the band gap into conduction band. Here the optical absorption is very small because there are relatively few trapped electrons compared with electrons in the valance band. Intraband transitions are property of metals only since the electrons move between energy states in the same band. In the various absorption processes, the electron and the holes absorb both a photon or a photon and a phonon. The photon supplies the required energy, whereas the phonon supplies the needed momentum. Therefore, the principal methods of determining the electron band structures of materials are optical methods. The relation between attenuation coefficient (absorption coefficient) and the extinction coefficient is given by:

$$k = \alpha\lambda/4\pi \tag{6}$$

7. Spectral distribution of the absorption coefficient: Direct and indirect band gaps determination

Study of the optical absorption edge in UV-region has proved to be very useful method for clarification of optical transitions and electronic band structure of the materials [15]. It is possible to determine indirect and direct transition occurring in band gap by optical absorption spectra at the fundamental absorption edge of the material. In both cases, electromagnetic waves interact with the electrons in the valance band, which are raised across the fundamental gap to the conduction band. In amorphous materials a different type of optical absorption edge is observed. In these materials, the absorption coefficient (α) increases with the photon energy near the energy gap.

Davis and Mott [16] gave an expression for the absorption coefficient, $\alpha(v)$, as a function of photon energy ($h\nu$) for

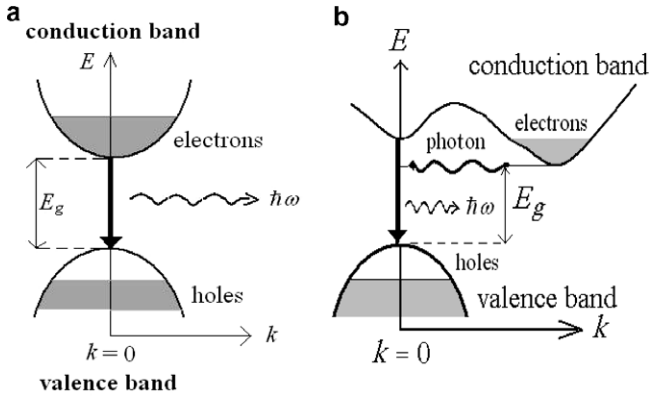

Fig. 3. Schematic diagram of the interband luminescence process in (a) direct gap semiconductor and (b) indirect gap.

direct and indirect optical transitions through the following,

$$\alpha(v) = \alpha_o\left(hv - E_g^{opt}\right)^n / hv \quad (7)$$

where the exponent $n = 1/2$ for allowed direct transition, while $n = 2$ for allowed indirect transition, see Fig. 3. α_o is a constant related to the extent of the band tailing, and E_g^{opt} is optical band gap energy.

The main feature of the absorption edge of amorphous materials is an exponential increase of the absorption coefficient with photon energy. When the energy of the incident photon is less than the band gap, the increase in absorption coefficient is followed with an exponential decay of density of states of the localized into the gap [17]. The absorption edge here is called Urbach edge, where α values are between 10 and $10^3\,cm^{-1}$. The lack of crystalline long-range order in amorphous/glassy materials is associated with a tailing of density of states into normally forbidden energy [17]. Urbach energy characterizes the extent of the exponential tail of the absorption edge. The exponential absorption tails and Urbach energy is given in accordance with the empirical relation [18]

$$\alpha(v) = \beta \exp(hv/E_U) \quad (8)$$

where β is a constant, E_U is the Urbach energy which indicates the width of the band tails of the localized states and (v) is the frequency of the radiation. The exponential absorption tails, i.e., Urbach energy depends on temperature, thermal vibrations in the lattice, induced disorder, static disorder, strong ionic bonds, and on average photon energies. The main factor contributing to edge broadening in crystalline materials is exciton–phonon coupling (dynamic disorder). In amorphous, an additional broadening due to static disordered exists. The Urbach role has been studies in detail both for crystalline [19] and glassy [19,20] forms of silica.

8. Inherent absorption wavelength and oscillator strength

Glass has generally an inherent absorption in the ultraviolet range. The inherent wavelength of the ultraviolet absorption or the average interband oscillator wavelength, λ_o, and the average oscillator strength, S_o, are determined using Drude-Voigt dispersion formula [21]. Cations can be classified into three groups according to the behavior of λ_o and S_o. The first group is characterized by small λ_o and large S_o values. In this group λ_o and S_o values increase with decreasing cationic field strength Z/a^2. Na^+, K^+, Mg^{2+}, and Ba^{2+} ions belong to this group. Values of λ_o and S_o of these glasses may be associated with the absorption of the non-bridging oxygen ions. The second group is characterized by extremely large λ_o and small S_o, where λ_o and S_o increase with decreasing Z/a^2. Bi^{3+}, Pb^{2+} and Tl^+ ions belong to this group. Values of λ_o and S_o of these glasses are considered to be associated with the absorption of cations themselves, which have $6S^2$ outer electrons. The third group cations are characterized by large value of λ_o and a smaller value of S_o than of the first group. In this group λ_o increases and S_o decreases with increasing Z/a^2. Cr^{3+}, Ti^{4+}, Zr^{4+}, Nb^{5+} and W^{6+} ions belong to this group.

9. Transition metals

The transition or *d*-block elements (such as Ti, V, Cr, Mn, Fe, Co, Ni, Cu, Zn, Zr, Ag, and Cd) are so called because their position in the periodic table is between the s- and p-block elements, and their properties transitional between the highly reactive metallic elements of the s block, which typically from ionic compounds, and the elements of the p block which are largely covalent. In the d-block the penultimate shell of electrons is being expanded from eight to eighteen by the addition of d electrons and typically the elements have an incompletely filled d level. Thus, all transition elements are metals and are good conductors of electricity and heat.

The covalent radii of the elements decrease from left to right across a row in the transition series, until near the end the size increases slightly. On passing from left to right, extra positive charges are placed on the nucleus and extra orbital electrons added. Since the d electrons shield the nuclear charge less efficient than the p electrons, hence the nuclear charge attracts the outer electrons more, and contraction in size occurs.

Ionic and covalent compounds of transition metals are colored in comparison to the s- and p-block elements which are almost always white. Color is associated with the ability to promote an electron from energy level to another. Exactly the right amount of energy to do this is obtained by absorbing the light of a particular wavelength. The d orbitals are not all identical in energy, and in the transition metals that have a partly filled d shell it is possible to promote electrons from one d level to another d level. This corresponds to a small energy difference, and so light is absorbed in the visible region. Ferric ions are coloring glass to be green while other coloring ions for glass are cobalt for blue, chromium for green, and manganese for purple.

One of the most striking features of the transition metals is that they exhibit variable valency (oxidation state) and

the valency changes in unit of one. When the transition metal ions are coordinated with other glass ions, the energy levels of the 3d electrons are split by the electric field of the coordinating ions. The d-electron orbitals are strongly directional, so the splitting is sensitive to the arrangement of the surrounding ions. Thus, transition metal ions are used to probe the glass structure and to study the coordination numbers of the central ions due to their outer d electron orbital functions have a broad radial distribution. The theory of these effects, called ''ligand field'' theory, was first developed by H. Bethe, and its application to glasses has been discussed in detail by Bates [22].

Ions with $3d^2$ configurations are interested in solid-state laser materials due to their ability to generate laser emission in the near infrared spectral region between 1.2 and 1.7 μm. In general, the presence of transition metal ions additives increases the refractive index and the transmission range at the expense of increasing the ultraviolet absorption.

Therefore many of the optical properties of oxide glasses and the effect of transition metals on their optical properties are briefly reviewed in this article. The article will be focused on the role of TiO_2 and Cr_2O_3, as transition metals, in the optical properties of some oxide glasses which have been prepared recently by the authors and by many other research groups.

10. Oxide glasses doped by TiO_2

Transparent glasses with non-linear refractive index, n_2, are widely investigated for future photonic applications such as ultra-fast switching and electro-optic modulators [23]. The resent discovery of second harmonic generation (SHG) in glasses after poling treatment and/or under high electric field induces new development related to functional integrated devices [24]. The choice of glass compositions is dictated by the necessity of increasing n_2 but various other parameters must be considered such as irradiation damage threshold for waveguides, fiber related devices and photonics. Oxide glasses containing proportions of TiO_2 have been reported. The empty d-shell Ti^{4+} metal ion is contributing to large increases of the linear and non-linear indices of the glasses [24,25], where titanium-oxygen entities are considered as the main factor contributing to hyperpolarizability of the glass.

Cardinal et al. [26] studied the glass local structure and optical non-linearity in poled oxide glasses of compositions $NaPO_3$–$Na_2B_4O_7$ and K_2O–SiO_2 which containing large proportions of TiO_2. They concluded that the increase in TiO_2 increases the hyperpolarizability which in turn increases the non-linear properties of the glasses.

Dimitrov and Komatsu investigated the rule of TiO_2 on electronic polarizability, optical basicity and optical non-linearity of oxide glasses [27]. It is found that the third-order non-linear optical susceptibility of the glasses increases with increasing optical basicity and tendency for metallization of the glasses. This is due to the high electron donor ability of TiO_2 and small optical band gap. Glasses with high refractive index show large polarizability, high optical basicity, small metallization criterion and large third-order non-linear optical susceptibility. They have also classified the oxide glasses using a polarizability approach taking into account the values of their refractive index-based oxide ion polarizability, optical basicity, metallization criterion, interaction parameter and ion's effective charges [28].

Le Boiteux et al. [29] studied the non-linear optical properties for TiO_2 containing phosphate, borophosphate and silicate glasses.

Hashimoto et al. [30] used Z-scan technique to measure the non-linear refraction and non-linear absorption of melt-derived and sol–gel-derived TiO_2-containing glass. The effects of composition and structure of glasses on the non-linear refractive index is measured. They found that a thermo-optic effect is present at TiO_2 content less than 25% and the titanium is the source of a positive Kerr effect. In TiO_2 range between 25 to 70 mol% a negative Kerr effect exist.

Zhu et al. [31] measured the non-linear refractive index n_2 of a PbO, TiO_2, SiO_2, and K_2O quaternary glass system by the laser beam longitudinal scanning Z-scan method and it is found to be 7.72×10^{-19} m^2/W and it is strongly correlated with the presence of more polarizable ions rather than the non-bridging oxygen content.

Zhu et al. [32] used Z-scan method to measure the non-linear optical properties for the PbO, TiO_2, K_2O, and SiO_2 system. The magnitude and sign of the non-linear refractive index n_2 were determined, as was the negative sign, which indicated a self-defocusing optical non-linearity. Two optical absorption bands at 540 and 660 nm, respectively, are observed in the optical absorption spectra. The sources of the absorption bands are attributed to the 3d-shell electronic transitions of Ti^{3+} ions from the ground state to the excited states. The origin of the negative non-linear refractive index was the contribution of resonant electronic transition processes, which can cancel the positive non-resonant refractive index that mainly resulted from the hyperpolarizabilities of the Pb–O and Ti–O pairs.

Shimoji et al. [33] measured the non-linear optical properties of Li_2O–TiO_2–P_2O_5 glasses by Z-scan technique using a nanosecond pulsed laser. The non-linear refractive index estimated from Z-scan normalized transmittance was considered to include the optical Kerr effect, the thermo-optic effect, and the resonant non-linearity related to Ti^{3+} ions of which content was increased with TiO_2 content. The sign of the thermo-optic effect for glasses with 5 and 10 mol% TiO_2 was positive, whereas for glasses with 15 and 20 mol% TiO_2 it was negative. The thermo-optic effect of all the glasses in this work was negative due to the negative temperature coefficient of linear refractive index (dn/dT), and decreased with increasing TiO_2 content, and was considered to be dominated by the two-photon absorption. For Ti^{3+}-containing $50Li_2O$–$15TiO_2$–$35P_2O_5$ glass with negative non-linear refractive index

(-1.78×10^{-18} m^2 W^{-1}), each of these three contributions was evaluated. The thermo-optic effect of the Ti^{3+}-containing glass was determined to be -22.11×10^{-18} m^2 W^{-1}. Using the non-linear refractive index and the thermo-optic effect for the Ti^{3+}-free glass made by remelting the Ti^{3+}-containing glass at 1000 °C under O_2 atmosphere, the optical Kerr of the Ti^{3+}-containing glass was found to be positive (11.87×10^{-18} m^2 W^{-1}). The resonant non-linearity of the Ti^{3+}-containing glass was found to be positive (8.46×1010^{-18} m^2 W^{-1}). As a result, it was concluded that negative non-linear refractive index of the Ti^{3+}-containing glass resulted from negative thermo-optic effect.

The Faraday effect, in which a rotation of the polarization plane of propagated light through media can by induced by a magnetic field in the direction of propagation, is closely related to dispersion theory and the Zeeman effect.

Tan and Arndt [34] monitored the Faraday Effect in TiO_2-SiO_2 glasses and the Verdet constants of silica and ULE glasses for wavelengths of 632.8 and 785 nm. The refractive index, wavelength-dependent Verdet constant of silica glass is calculated from 213.856 to 6725 nm with the derived equation by means of the dispersion theory. For silica glass, the evaluated Verdet constants for wavelengths of 632.8 and 785 nm were found to be $(3.930 \pm 0.017) \times 10^{-6}$ and $(3.237 \pm 0.068) \times 10^{-6}$ (rad/A), respectively. The Verdet constants of ULE glass (Corning, Code 7971) at 632.8 and 785 nm were $(3.836 \pm 0.064) \times 10^{-6}$ and $(3.297 \pm 0.073) \times 10^{-6}$ (rad/A), respectively.

Optical absorption properties of TiO_2-doped and non-doped silica glass were studied by Yano and Morimoto to investigate the effect of titanium (Ti) ion doping on absorption spectra changes produced by 7.2 eV irradiation [35]. The samples were prepared by polishing down to a thickness of about 100 μm to resolve the absorption bands in the VUV range and to measure the color center created or eliminated in the irradiated surface region. For both kinds of silica glass, the magnitude of the 7.6 eV absorption band of a thin sample (<100 μm) decreased at the early stage of irradiation, while that of the 5.8 eV absorption band increased. In the thick sample (>100 μm), the 7.6 eV band magnitude increased even in the early stages of irradiation. These results indicate that the silica glass absorbs <7 eV light, which is much smaller than band gap energy of SiO_2 glass, and produces ≡Si–Si≡ bonds. The magnitudes of these changes were smaller in the TiO_2-doped silica glass. The molar extinction coefficients of TiO_2 in silica glass were determined in the 4.0–8.0 eV range by using 47–150 wt ppm Ti containing samples. To avoid perturbation by absorption due to ≡Si–Si ≡ bonds, the samples were heated at 950 °C in hydrogen atmosphere. Two absorption maxima were observed at 6.2 and 7.6 eV, and the corresponding molar extinction coefficients were estimated to be 3.0×10^4 and 5.5×10^4 L mol^{-1} cm^{-1}, respectively. The absorption, 7.6 eV, in the TiO_2 doped samples prevents bond breaking by VUV photon for silica glass.

Nonlinear optical glasses with fast response times and very low absorption coefficients are promising materials for use in ultra-fast (picosecond) all-optical switches. Vogel et al. [36] reported a relatively high third-order optical non-linearity in equimolar TiO_2–Nb_2O_5–B_2O_3–Na_2O–SiO_2 glass. The non-linear index coefficient n_2 for this glass composition was found to be 4×10^{-19} m^2/W. In order to determine the relationship of the various physical properties to the structure and/or composition in these glasses, they have synthesized series of glasses in the four-component TiO_2–Nb_2O_5–Na_2O–SiO_2 system. Their structures have been studied by Raman spectroscopy, and their linear refractive indices and non-linear index coefficients were measured. The data show that the linear refractive index is mainly determined by the total concentration of Ti + Nb, whereas the non-linear index coefficient is much larger for Ti than for Nb doping. The combined presence of Ti and Nb extends the glass forming region in this system.

Xiang et al. [37] reported an up-conversion emission in violet (408 nm) from Nd^{3+}-doped $93SiO_2$:$7TiO_2$:$20AlO_{1.5}$ glasses synthesized by the sol–gel process. Upon excitation at 583 nm ($^4I_{9/2} \rightarrow {}^4G_{5/2}$), a bright violet up-conversion emission at 408 nm has been observed. The behavior of the up-conversion luminescence has been compared with that of the normal luminescence at both 408 and 1064 nm. The results show that while no concentration quenching for up to 2 mole Nd content is observed for the up-conversion emission, such an effect can be observed for the normal luminescence cases. Although the up-conversion luminescence has a shorter lifetime and weaker intensity, it is of use to the development of sol–gel glass-based waveguide lasers operating at the violet wavelength.

Martinet et al. [38] deposited silicon dioxide and titanium dioxide films at low temperature by electron cyclotron resonance (ECR) plasma enhanced chemical vapor deposition (PECVD) using respectively O_2 and tetraethoxysilane (TEOS) or titanium isopropoxide (TIFF) as precursors. To control the thickness and the refractive index during deposition, the plasma reactor was equipped with an in situ spectroscopic ellipsometer. Deposition kinetics and layer properties were investigated by spectroscopic ellipsometry, X-ray photoelectron spectroscopy (XPS) and chemical etch rate. A double film antireflection coating was fabricated and reflectance was measured using a UV–visible near-infrared spectrometer. Results reported demonstrate that deposition of SiO_2 and TiO_2 films at low temperature by PECVD is a promising method to produce antireflection coatings for solar cells.

Second harmonic generation in poled glasses is reported with $(1-x)LaMgB_5O_{10}$–$xTiO_2$ and $(1-x)LaMgB_5O_{10}$–xNb_2O_5 ($0 \leqslant x \leqslant 0.4$) glasses by Nazabal et al. [39]. Optical properties of transmission like linear refractive indexes and third-order non-linear optical susceptibility have been investigated. A second harmonic signal was observed for each thermally poled composition, except for the $LaMgB_5O_{10}$ matrix glass.

El-Alaily and Mohamed [40] studied the optical properties including infrared and refractive index and density of lithium borate glass as a base glass. The effect of the

presence of either aluminum or lead oxide, or the presence of one of the following transition metal, Fe_2O_3, TiO_2 or V_2O_5 was investigated. The effect of exposing the glass to either gamma, or fast neutron irradiation on the last properties was also studied. The results showed that three main bands appeared due to bending vibration or stretching of either, tetrahedral or triagonal borate units. The addition of alkalis causes only a shift of the bands either to higher or lower wavelength. Glass containing lead oxide had the highest refractive index and density, also the presence of any of the transition metal oxide lowering the average coordination number of oxygen which causes a compaction of the structure hence an increase in the values of density and refractive index. Since irradiation of glass causes compaction of B_2O_3 by breaking the bonds between triagonal elements, the average ring size becomes smaller which leads to an increase in density and refractive index too.

Hauch et al. [41] developed a new photoelectrochromic device with excellent coloring and bleaching characteristics. In contrast to other photoelectrochromic devices, the electrochromic layer (e.g. WO_3) and the photoactive layer (e.g., dye-covered TiO_2) are situated on the same TCO-coated glass substrate (TCO: transparent conductive oxide). The opposing electrode is a platinized TCO-coated glass. The electrolyte contains Li^+ and a redox couple (I^- and I_3^-) in an organic solvent (e.g. propylene carbonate). Under illumination, the electrochromic layer is colored, and in the dark it is bleached. The advantage of this new device is that a catalyst (Pt) can accelerate the bleaching process independently of the coloration process. Thus a deep and fast coloration, and fast bleaching, can be achieved in the same device. The coloration is fast even for large areas, because the TCO is not necessary for the coloration process. Under 1 sun of illumination, they measured a transmittance change from 64 to 23% in 2 min. The bleaching time is about 2 min.

Pure and doped niobium oxide (Nb_2O_5) layers are electrochromic (EC) materials which change their color by insertion of Li^+ ions from transparent to brown, grey or blue depending on the crystallinity of the layer. Heusing et al. [42] produced EC-devices with the configuration K-glass/EC-layer/composite electrolyte/ion-storage (IS) layer/K-glass, using different Nb_2O_5 EC-layers, a $(CeO_2)_x(TiO_2)_{1-x}$ ($x = 0.45$) IS-layer and an inorganic–organic composite electrolyte to which a small amount of water (up to 3 wt.%) was added. The grey coloring all-solid-state sol–gel devices fabricated with Nb_2O_5:Mo coatings show a high reversible coloration (DOD = 0.3) and a long-term stability of more than 55 000 switching cycles. Large area EC-devices (30×40 cm) show a transmittance change between 60% and 25% at 550 nm after galvanostatic coloration and bleaching for 3 min and a coloration efficiency of 27 cm^2/C. The results obtained with blue and brown coloring Nb_2O_5 EC-layers and a comparison with blue coloring WO_3 layers are also presented.

Rao et al [43] prepared AF–PbO–B_2O_3 (where A = Li, Na, K) glasses containing different concentrations of TiO_2 ranging from 0 to 0.6 mol%. A variety of spectroscopic studies viz. infrared spectra, optical absorption, ESR spectra and thermoluminescence have been carried out as a function of titanium ion concentration. The results of these studies have been analyzed in the light of different oxidation states of titanium ions. The comparison of the results of three series indicates the lithium series glasses are the better candidates for the practical applications.

Villegas and Navarro determined the glass forming region in the TeO_2–TiO_2–Nb_2O_5 ternary system [44]. The structural role of each component was studied by FTIR and some of their physical properties (density, molar volume, oxygen molar volume, transition temperature, thermal expansion coefficient, optical absorption and energy gap) were determined. The glass structure is mainly built by [TeO_4] groups, while Nb^{5+} and Ti^{4+}-ions play as network modifiers. As the Nb_2O_5 and TiO_2 concentration increases, [TeO_4] groups progressively change to [TeO_3] groups as a consequence of the network opening. The contribution of the three ions to the oxygen molar volume follows the order: $Te^{4+} > Ti^{4+} > Nb^{5+}$. TiO_2 incorporation and even more Nb_2O_5 improve the glasses thermal stability and the network reinforcement. TiO_2 is the component which contributes in the highest extent to decrease the glass energy gap.

Boye et al. [45] used monolithic Er-doped SiO_2–TiO_2 binary glasses of high optical quality in an investigation of the effects of different annealing conditions and titanium content on fluorescence yields and decay times of the $^4S_{3/2}$ level of Er^{3+}. In addition, the characteristics of green upconverted fluorescence from the $^4S_{3/2}$ level via excitation with red laser light (655 nm) were studied. Energy transfer up-conversion involving two ions in the $^4I_{11/2}$ state was determined to be the dominant up-conversion mechanism. The glasses with TiO_2 showed enhanced up-conversion and required lower annealing temperatures for the up-conversion to be observed when compared to SiO_2 glasses doped with Al.

Toyohara et al. [46] prepared the transparent nanocrystallized (heat-treatment: 750 °C, 1 h) glasses consisting of ferroelectric $Ba_2TiSi_2O_8$ nanocrystals (size: 100–200 nm) in $40BaO$–$20TiO_2$–$40SiO_2$ glass, and the effect of a thermal poling (DC electric voltage: 8.8 kV/cm, temperature: 110–300 °C, time: 1 h) on the second harmonic (SH) intensity has been examined. It is found that the formation behavior of nanocrystals at the surface differ from that in the interior of glass, giving a new insight into the well-known concept for nanocrystallization or homogeneous nucleation in glass. The Maker fringe patterns with fine structures are observed, indicating a high orientation of the polarization axes of $Ba_2TiSi_2O_8$ crystals formed at the surface. The prominent enhancement in the SH intensity is observed due to thermal poling, demonstrating that thermal poling is an effective method in enhancing anisotropic polarization of ferroelectric $Ba_2TiSi_2O_8$ nanocrystals in crystallized glasses. The giving study proposes that the Maker fringe pattern for SH intensity of nanocrystallized glasses is very sensitive to the anisotropic polarization of nanocrystals at the surface,

indicating the importance of the Maker fringe technique for the characterization of nanocrystals in materials.

Masai et al. [47] examined the $BaO–TiO_2–SiO_2$ crystallized glass containing $Ba_2TiSi_2O_8$ crystal phase using X-ray diffraction (XRD) measurement and Maker fringe technique. It has been found that the crystallized glasses with a composition of close to the stoichiometric $Ba_2Ti–Si_2O_8$ showed bulk crystallization, whereas other crystallized glasses with non-stoichiometric composition of $Ba_2Ti–Si_2O_8$ showed surface crystallization. The parameter ΔT, the difference in temperature between the crystallization onset and the glass transition temperature, strongly affects the crystallization behaviors of the present BTS glasses. The $30BaO–20TiO_2–50SiO_2$ transparent surface crystallized glass with strong c-oriented $Ba_2TiSi_2O_8$ phase showed its second-order non-linear optical constant, $d_{33} = 6.1$ pm/V.

Raghavaiah et al. [48] prepared $PbO–Sb_2O_3–As_2O_3$ glasses containing small concentrations of TiO_2 ranging from 0 to 0.5 mol%. A number of studies viz. differential scanning calorimetry, infrared spectra, optical absorption, ESR spectra and magnetic susceptibility have been carried out as a function of titanium ion concentration. The interesting changes observed in these properties are discussed in the light of different oxidation states of titanium ions.

Rao et al. [49] prepared $Li_2O–MgO–B_2O_3$ glasses containing different concentrations of TiO_2 (ranging from 0 to 1.0 mol.%). A number of studies namely dielectric properties (constant ε', loss $\tan\delta$ and AC conductivity σ_{ac} as in the frequency 10^2–10^5 Hz and in temperature range 30–300 °C), optical absorption, ESR, magnetic susceptibility, thermoluminescence and infrared spectra were carried out on these glasses. Results have been analyzed in the light of different oxidation states of titanium ions in the glass matrix.

Kosaka et al. [50] prepared ternary $BaO–TiO_2–B_2O_3$ glasses containing a large amount of TiO_2 (20–40 mol%), and their optical basicities (Λ), the formation, structural features and second-order optical non-linearities of $BaTi(BO_3)_2$ and $Ba_3Ti_3O_6(BO_3)_2$ crystals are examined to develop new non-linear optical materials. It is found that the glasses with high TiO_2 contents of 30–40 mol% show large optical basicities of $\Lambda = 0.81$–0.87, suggesting the high polarizability of TiO_n polyhedra ($n = 4$–6) in the glasses. $BaTi(BO_3)_2$ and $Ba_3Ti_3O_6(BO_3)_2$ crystals are found to be formed as main crystalline phases in the glasses. It is found that $BaTi(BO_3)_2$ crystals tend to orient at the surface of crystallized glasses. The new XRD pattern for the $Ba_3Ti_3O_6(BO_3)_2$ phase is proposed through Rietvelt analysis. The second harmonic intensities of crystallized glasses were found to be 0.8 times as large as α-quartz powders, i.e., $I^{2\omega}(\text{sample})/I^{2\omega}$ (α-quartz) = 0.8, for the sample with $BaTi(BO_3)_2$ crystals and to be $I^{2\omega}(\text{sample})/I^{2\omega}$ (α-quartz) = 68 for the sample with $Ba_3Ti_3O_6(BO_3)_2$ crystals. The Raman scattering spectra for these two crystalline phases are measured for the first time and their structural features are discussed.

Westin et al. [51] investigated the possibility of avoiding formation of Er-rich oxide clusters in $ErAl_3O_6–TiO_2–SiO_2$ glassy films. Samples containing 0.5, 1, and 3 mol% Er^{3+} were prepared using a precursor with a single, isolated Er-ion, $ErAl_3(OPr^i)_{12}$, in the metal–organic sol–gel route. The thermal decomposition of the gel films to form amorphous oxide films was studied by thermogravimetry, Fourier transform infrared spectroscopy (FT-IR), powder X-ray diffraction and by means of a transmission electron microscope, equipped with an energy dispersive spectrometer. The microscopy studies of the oxide films obtained after 2 h at 900 °C showed that they were amorphous and free of Er-rich clusters. The optical and vibrational properties of the glasses were studied using FT-IR, Raman scattering and luminescence spectroscopy. The samples exhibit luminescence both in the visible and IR under excitation of the 514.5 and 488 nm Ar^+ laser lines. The emission around 1.5 μm was maximum for the 1 mol% sample. The results show that the preparation technique can produce samples with an unusually large amount of Er doping, before Er-clustering induced quenching of the luminescence appears. Up-converted emission was also detected around 21 000 and 24 500 cm^{-1}.

Vithal et al. [52] investigated the optical and electrical properties of the lead bearing glasses in the $PbO–TiO_2$, $PbO–TeO_2$, and PbO–CdO systems. The density, refractive index, optical band-gap, and Urbach energies of these glasses are reported. It is shown that the additive nature of oxide ion polarizabilities reported for the simple oxides can be extended to glass systems as well. A modified linear relationship between $(E_{opt})^{1/2}$ and $1-(Rm/Vm)$ holds good for glasses. The oxide ion polarizabilities deduced from two different experimental quantities viz., refractive index and optical band-gap energy agree well. The dc electrical conductivities have been measured in the temperature range 350–700 K. The activation energies are close to 1 eV. The low melting $70PbO–30TeO_2$ glass shows higher isothermal conductivity compared to other glasses of similar composition. In $PbO–TiO_2$ glass the PbO content contributes significantly to conductivity and composition dependence of pre-exponential factor (σ_0) supports tunneling mechanism.

Karlsson and Liu [53] prepared 15 high titania glasses in the system $Li_2O–Na_2O–MgO–CaO–TiO_2–ZrO_2–SiO_2$ and their refractive indices, dispersions and densities are determined. Polynomial models were derived to describe the relationships between properties and glass composition. The refractive index and dispersion models were linear, while the density model required second degree terms for an adequate fit to experiments.

Su and Deng [54] prepared Tm^{3+}/Yb^{3+} co-doped tellurite glasses with the base compositions (in mol%) $80TeO_2–10\,K_2O–(9.9-x)TiO_2–0.1Tm_2O_3–xYb_2O_3$ ($x = 0.1$, 0.3, 0.5, 1.5 and 2.0) by the conventional melting method, and their absorption spectra were performed, and their indirect sensitization upconversion spectra were studied in detail. It was interesting to note that the luminescence peaks of

indirect sensitization upconversion excited by 800 nm laser diode varied from 475 nm to 452 nm at first, then to 468 nm with x increasing, the corresponding luminescence intensity also increased with x. The processes of indirect sensitization upconversion were analyzed in detail. The upconversion efficiency increased greatly, the efficiency of the sample when $x = 2.0$ was nearly 20-fold of that sample $x = 0.1$.

Takahashi et al. [55] examined second-order optical non-linearities for the transparent $Ba_2TiGe_2O_8$ (BTG) crystallized glasses with the composition of $40BaO \cdot 20TiO_2 \cdot 40GeO_2$ (BTG40), $33.3BaO \cdot 16.7TiO_2 \cdot 0GeO_2$ (BTG50) and $30BaO \cdot 15TiO_2 \cdot 55GeO_2$ (BTG55). A very large d_{33} value for a transparent BTG crystallized glass in BTG55 was achieved, i.e., $d_{33} = 22 \pm 3$ pm/V, being comparable to that of $LiNbO_3$ single crystal. The d_{33} for BTG50 and BTG40 were measured to be 12 ± 3 pm/V and 7 ± 2 pm/V, respectively. This result indicates that d_{33} decreases with GeO_2 concentration, when approaching the glass composition of the stoichiometric BTG crystal. For a larger d_{33} value in BTG crystallized glasses, it is considered that the high homogeneity of the oriented surface $Ba_2TiGe_2O_8$ crystalline layer on the crystallized BTG55 glass is accomplished by a suitable amount of benitoite phase of $BaTiGe_3O_9$, which acts a nucleation site for the BTG crystal.

Feitosa et al. [56] prepared partially crystallized glasses containing non-centrosymmetric b-BaB_2O_4 (b-BBO) and/or $BaTi(BO_3)_2$ crystals by controlled surface crystallization of x_1TiO_2–x_2BaO–$x_3B_2O_3$ glasses, where $x_1 = 4\%$, 8%, 15% and $x_2/x_3 = 8/9$ (mol%). Differential thermal analyses were made to select appropriate heat treatments to partially crystallize some samples. The resulting crystalline phases were determined by X-ray diffraction and micro-Raman spectroscopy. Spontaneous preferred orientation (texture) occurred on the surface of all these glasses. Samples with $x_1 = 4\%$ and 8% heat-treated from 1 to 32 h showed only b-BaB_2O_4 precipitated on the glass surfaces, while the glass with $x_1 = 15\%$ only had $BaTi(BO_3)_2$ in samples heat-treated for less than 8 h. Longer treatments also led to crystallization of b-BaB_2O_4, occurring preferentially between the arms or underneath the $BaTi(BO_3)_2$ crystals, but present on the glass surface as well, and this became the predominant crystalline phase. Some surface crystallized glasses yielded a reasonable second-harmonic generation. The non-linear optical coefficient, d_{eff}, in the $x_1 = 15\%$ crystallized sample was 1.1 pm/V, which corresponds to approximately 50% of that observed in the b-BBO single crystal.

Abdel-Baki et al. [57] prepared different $x TiO_2$–$(60 - x)SiO_2$–$40Na_2O$ ($0 \leqslant x \leqslant 20$ wt%) glasses in the form of plane parallel slabs. The optical constants of these optical glasses are determined over a wide spectral range, 0.2–3 μm, providing the complex dielectric constant to be calculated. The different dispersion parameters of the studied compositions are determined as well. Higher values for the refractive index and dispersion are recorded due to the high polarizability of Ti and the low preference of 4-coordination for titanium. The wavelength for zero material dispersion is evaluated. The second-order index of refraction and the third-order non-linear optical susceptibility are computed from the measured linear refractive index data. These non-linear properties of the present glass show one order of magnitude enhancement over some TiO_2 silicate glasses. The measured mid-IR-spectra of the different glasses are carried out to investigate the structure of the present glasses. It has been found that, the addition of titanium (i.e., highly polarizable element) not only act as glass modifier but behaves as intermediate and Ti^{4+} exalts more the measured glass parameters.

Abdel-Baki et al. [58] determined different optical properties of $x TiO_2$–$(60 - x)SiO_2$–$40Na_2O$ ($0 \leqslant x \leqslant 20$ wt%) optical glasses. The characterization is done over a wide energy range, 0.41–6.2 eV. The refractive index and the extinction coefficient data are used to measure the absorption coefficient of the different glass compositions. Studying the UV absorption edge, both direct and indirect allowed transitions with their optical energy gaps are carried out. In the same time, the Urbach energy is evaluated. From the extinction coefficient data, the Fermi energy of the glasses is calculated. The molar refraction, electronic polarizability and the optical basicity are obtained using the measured glass refractive indices.

Astilean et al. [59] proposed the use of high-index materials for the fabrication of subwavelength diffractive components operating in the visible domain. This approach yields a reduction of fabrication constraints and an improvement of theoretical performance. A blazed grating with subwavelength binary features and with a period of 5.75 wavelengths is designed and fabricated in a TiO_2 layer coated upon a glass substrate. The first-order diffraction efficiency measured with a He–Ne laser beam is 83%, which is slightly larger than that achieved theoretically by the best standard (continuous profile) blazed grating fabricated in glass with the same period.

11. Oxide glasses doped by Cr_2O_3

Sharonov et al. [60] presented a spectroscopic study of transparent forsterite nanocrystalline glass–ceramic doped with chromium, a promising active medium for near-infrared fiber-optic applications. Absorption, emission, excited-state absorption spectra, and continuous function decay analysis of luminescence decay reveal the presence of Cr^{3+} and Cr^{4+} centers in both glass and crystal phases. The optical behavior of Cr^{3+} and Cr^{4+} centers is discussed and compared with that in bulk forsterite crystals.

Aluminum oxide waveguides are doped with erbium for applications in telecommunication to develop an integrated optical amplifier [61]. Also Al_2O_3 doped with transition elements to develop tunable solid state lasers for spectroscopic measurements is of interest. Lasers with broadest fluorescence bands are Ti:Sapphire lasers or chromium doped specific crystals or glasses. In this paper the suitability of titanium and chromium doped aluminum oxide

material as laser material is examined. Titanium and chromium doped waveguides have been annealed. Their fluorescence and lifetime measurements are presented.

Ravikumar et al [62] carried out EPR and optical absorption investigations of chromium doped cadmium phosphate glass. Crystal field, spin-Hamiltonian and bonding parameters are evaluated. From the results and analyses of the EPR and optical studies, the site symmetry of Cr^{3+} ion in the glass is ascribed to a distorted octahedron. The bonding parameters suggest the ionic nature of Cr^{3+} ion with the ligands.

There is considerable interest in compact pulsed high peak power laser sources emitting at wavelengths near 1.55 μm. Rangefinders and other applications with free space propagation could be a benefit of such devices. The wavelength of around 1.55 μm is in the eye safe regime where significantly higher pulse energies can be used without damaging human eyes. Erbium- and ytterbium-doped YAG single crystals were obtained by the Czochralski method. The basis conditions of growth and the results of optical homogeneity measurements of the obtained crystals are presented [63]. This report describes also the effect of variations of erbium, ytterbium, chromium ions and glass base compositions on laser efficiency and the improved properties of a new glass base. The spectral properties and laser characteristics were investigated. Absorption spectra of Er^{3+} and Yb^{3+}-doped active media were measured in the spectral range 190–5000 nm at room temperature. Excitation and luminescence spectra were also recorded at room temperature with a Jobin-Yvon spectrofluorometer using a diode laser (Polaroid 4300, 980 nm, 1 W) as an excitation source. The measurements of the lifetime of the Er^{3+} ions in the upper laser level ($^4I_{13/2}$) of the samples were made by the direct method with pulse excitation.

El-Hadi [64] studied the optical absorption of some selected high-lead borate glasses containing chromium exposed to different doses of gamma irradiation. The results obtained showed that the absorption bands before and after irradiation exhibited changes with the radiation dose and chemical composition of the glass. The response of the glass to gamma irradiation was related to the creation and spread of defects "color centers," the approach of a saturation condition after a certain irradiation dose, and the possible photochemical effect on the transition metal present in the glass.

Munin et al. [65] prepared chromium-doped aluminate and silicate glasses in both inert and oxidizing atmospheres. Spectroscopic measurements indicate that some of the glasses incorporated the chromium ion in the 4+ valence state. These Cr^{4+} doped glasses exhibit a broad spectral emission covering the communication window and the eye safe region around 1.5 μm. Ten glass samples and two crystalline materials were used to study the phenomenon of saturable absorption in the Cr ion. A figure of merit was defined to compare the performance of different materials as saturable absorbers. The preparing conditions that lead to a glass saturable absorber with better figure of merit have been investigated. A Q-switched Cr:LiSAF laser was used for the saturable absorption measurements.

The optical and structural characteristics of sol–gel SiO_2 powders and coatings containing Cr are reported [66]. The samples were characterized using X-ray diffraction, micro-Raman, visible photoacoustic absorption spectroscopy (PAS), optical transmission spectroscopy and diffuse reflectance. Glasses with a wide range of colors were obtained either by varying the chromium concentration, in the range of 0.1–20% w/w, or by air heat treatments in the range of 100–500 °C. These optical changes are explained in terms of the different chemical states adopted by the Cr into the SiO_2 matrix. Three absorption bands at 370, 460 and 600 nm were observed in the PAS, diffuse reflectance and optical transmission measurements. According to the ligand field theory, the last two bands are identified with electronic transitions in the d–d levels of Cr^{3+}; these two bands are better defined in the PAS measurements. The band at 370 nm, due to a ligand-to-metal charge transfer, in which chromium has the Cr^{6+} valence state, is only observed using optical transmission measurements. X-Ray measurements show the formation of Cr_2O_3 particles only in the samples with 20% w/w of Cr after annealing at 500 °C. The Raman spectra are not sensitive to the chromium oxide particles, but reveal the existence of isolated chromate- and dichromate-like structures.

Grinberg [67] presented a review of recent investigations on disordered materials such as glasses and disordered crystals doped with chromium. The main goal of the research was the determination of the lattice disorder and the influence of this disorder on the properties of the luminescence centers and the non-radiative processes. The most important and novel are theoretical approaches that allow recovery of the distribution of the lattice disorder and the crystal-field parameters from the spectroscopic data.

Tanaka et al. [68] examined the crystallization process of sodium indium borosilicate glasses doped with Cr^{3+}. $InBO_3$:Cr^{3+} precipitates as a single phase from $26.85Na_2O$–$44.75B_2O_3$–$17.9SiO_2$– $10In_2O_3$–$0.5Sb_2O_3$–$0.1Cr_2O_3$ glass. A comparison of fluorescence spectra between glass-ceramic and polycrystalline $InBO_3$:Cr^{3+} indicates that Cr^{3+} is incorporated in the $InBO_3$ phase in the glass–ceramic specimen. Optical absorption and fluorescence measurements reveal that Cr^{3+} ions occupy sites with high ligand fields in the glass whereas the ligand field strength of Cr^{3+} ion site in the $InBO_3$ crystal is low; the ligand fields of sites for the Cr^{3+} ions vary from high to low states with the crystallization of the glass. This trend is opposite to a tendency usually observed in the precipitation process of crystals doped with Cr^{3+} from oxide glasses. The origin for the high ligand field in the sodium indium borosilicate glass is speculated by considering the role of In^{3+} ions in the glass structure.

Felice et al. [69] prepared chromium-doped, silica-based performs and optical fibers by modified chemical vapor

deposition (MCVD) and have studied the influence of the chemical composition of the doped region on the Cr-oxidation states and the spectroscopic properties of the samples. Chromium, introduced initially as Cr^{3+}, is partially or totally oxidized during the fabrication process, and is stabilized in the core of the performs and fibers as Cr^3 in octahedral coordination, and/or as Cr^{4+} in distorted tetrahedral coordination (C_s). Small concentrations (~1–2 mol%) of codopants in silica, such as germanium or aluminum, suffice to promote a particular oxidation state. Particularly, 1 mol% of aluminum stabilizes all the present chromium into Cr^{4+} The ligand field parameters, Dq, B and Dq/B, for Cr^{3+} and Cr^{4+} are derived. It is shown that the chromium ions in our samples are in low-to- intermediate ligand field and that Dq and Dq/B decrease when the aluminum content increases. The absorption cross-section of Cr^{3+} similar to those reported in glasses and crystals, whereas Cr^{4+} has lower values than the reference laser materials.

Jiang et al. [70] prepared phosphate glass samples with various Cr_2O_3, Yb_2O_3, and Er_2O_3 contents based upon $67\ P_2O_5 \cdot 4Al_2O_3 \cdot 14Li_2O.1\ K_2O \cdot 4(Yb_2O_3 + Er_2O_3)$. The effect of changing concentrations of Er^{3+} ions ($0.1–1.5 \times 10^{19}$ ions cm^{-3}) and sensitizers Cr^{3+} ion and Yb^{3+} ion ($2–16 \times 10^{18}$ ions cm^{-3} and $1.35–2.3 \times 10^{21}$ ions cm^{-3}, respectively) on laser performance were investigated. The thermal shock resistance of this glass was doubled after an ion-exchange chemical strengthening process in a $KNO_3/NaNO_3$ molten salt bath. Lasers with repetition rates of 20 Hz at free-running and 15 Hz at Q-switched single mode were demonstrated by utilizing chemically strengthened laser glass rods.

Optical absorption, thermoluminescence, infrared spectra and differential thermal analysis of three different tellurite glass systems viz., $ZnF_2–As_2O_3–TeO_2$, $ZnF_2–Bi_2O_3–TeO_2$ and $ZnF_2–P_2O_5–TeO_2$ containing 0.4% of Cr_2O_3, have been investigated [71]. Results have been analyzed in the light of different oxidation states of chromium ion and the most suitable host for lasing Cr^{3+} ions has been identified and reported.

Durga and Veeraiah [72] prepared clear glasses of the system, $ZnF_2–As_2O_3–TeO_2$, containing different concentrations of Cr_2O_3 (ranging from 0 to 0.6 wt%). A number of studies viz., differential thermal analysis, infrared spectra, optical absorption, ESR, magnetic susceptibility, thermoluminescence and dielectric properties (constant ε; loss tan δ; AC conductivity σ_{AC} over a range of frequency and temperature and dielectric breakdown strength), on these glasses were carried out as a function of chromium ion concentration. Results have been analyzed in the light of varying oxidation states of chromium ion; the analysis indicates a gradual conversion of chromium ions from Cr^{3+} state to Cr_4^{2-} structural units (that take part in network-forming positions) in the glass network, when Cr_2O_3 is present at higher concentrations (>0.3 wt%) in the glass matrix.

Rao and Veeraiah [73] investigated the optical absorption, ESR, infrared spectra, thermoluminescence, differential thermal analysis and dielectric properties of $R_2O–CaF_2$-B_2O_3 ($R_2O = Li_2O$, Na_2O, K_2O) glasses containing 0.4% of Cr_2O_3. Results have been analyzed in the light of different oxidation states of chromium ion. The analysis indicate the presence of a part of the chromium ions in the Cr^{6+} state adopting network-forming positions in $Li_2O–CaF_2–B_2O_3$ glasses whereas in $K_2O–CaF_2–B_2O_3$ glasses these ions mostly exist in the Cr^{3+} state acting as modifiers.

Strek et al. [74] presented the results of EPR and optical measurements of Cr-doped silica glasses obtained by means of sol technology. The effect of Cr concentration on optical behavior was studied. Thermoluminescence was observed after heating previously cooled and UV irradiated samples. The EPR measurements were performed for UV irradiated samples and a strong temperature dependence of the signal was noticed. The nature of optically active Cr centers was discussed. It is concluded that the EPR signal is associated with Cr^{5+} ions at tetrahedral sites whereas the emission is attributed to the ligand-metal charge transfer transitions of Cr^{6+} ions coupled to Cr^{5+}. No evidence was found for the presence of Cr^{3+} ions in silica gel glass.

El-Diasty et al. [75] prepared series of new Lithium Aluminum Silicate (LAS) glass systems doped with chromium ion. The reflectance and transmittance of the glass slabs are recorded. By means of an iteration procedure, the glass refractive index, n, and the extinction coefficient, k, and their dispersion are obtained. Across a wide spectral range, 0.2–1.6 μm, the dispersion curves are used to determine the atomic and quantum constants of the prepared glasses. These findings provide the average oscillator wavelength, the average oscillator strength, oscillator energy, dispersion energy, the lattice energy and material dispersion of the glass materials to be calculated. For optical waveguide applications, the wavelength for zero material dispersion is obtained. Dilatometric measurements are performed and the thermal expansion coefficient is calculated to throw some light on the thermo-optical properties of the present glasses correlating them with their structure and the presence of non-bridging oxygen ions.

El-Diasty et al. [76] prepared Lithium Aluminum Silicate glass system (LAS) implanted with chromium ions. The reflectance and transmittance measurements are used to determine the dispersion of absorption-coefficient. The optical data are explained in terms of the different oxidation states adopted by the Chromium ions into the glass network. It is found that the oxidation state of the chromium depends on its concentration. Across a wide spectral range, 0.2–1.6 μm, analysis of the fundamental absorption edge provides values for the average energy-band gaps for allowed direct and indirect transitions. The optical absorption coefficient just below the absorption edge varies exponentially with photon energy indicating the presence of Urbach's tail. Such tail is decreased with the increase of the Chromium dopant. From the analysis of the optical absorption data, the absorption peak at ground state exciton energy, the absorption at band gap and the free

exciton binding energy are determined. The extinction coefficient data is used to determine the Fermi energy level of the studied glasses. The metallization criterion is obtained and discussed exploring the nature of the glasses. The measured IR-spectra of the different glasses are used to throw some light on the optical properties of the present glasses correlating them with their structure and composition.

References

[1] Zachariasen WH. J Am Chem Soc 1932;54:3841.
[2] Goldschmidt VM. Skrifter Norske Videnskaps Akad (Oslo). Mat Natur 1926;1:7.
[3] Stanworth JE. J Am Ceram Soc 1971;54:61.
[4] Warren BE, Biscoe J. J Amer Ceram Soc 1938;21:49.
[5] Mysen BO. Structure and properties of silicate melts. Amsterdam: Elsevier; 1988.
[6] Jiang N, Qiu J, Silcox J. Appl Phys Lett 2000;77:3956.
[7] Abdel-Baki M, Abdel-Wahab FA, Radi A, El-Diasty F. J Phys Chem Solids; in press;68:1457.
[8] Lee JD. A new concise inorganic chemistry. London: Van Nostrand Reihhold; 1977.
[9] Duffy JA, Ingram MD. In: Uhlman D, Kreidl N, editors. Optical properties of glass. Westerville: American Ceramic Society; 1991.
[10] Duffy JA. Geochim Cosmochim Acta 1993;57:3961.
[11] Boyed Robert W. Nonlinear optics. Academic Press; 1992.
[12] Vogel EM, Weber MJ, Krol DM. Phys Chem Glasses 1991;32:231.
[13] Boyed Robert W. Nonlinear optics. Academic Press; 1992.
[14] Boling NL, Glass AJ, Owyoung A. IEEE J Quant Elec 1978;QE-14:601.
[15] Mott NF, Davis EA. Electronic processes in non-crystalline materials. Oxford: Clarendon Press; 1979.
[16] Davis EA, Mott NF. Phil Mag 1970;22:903.
[17] Abay B, Guder HS, Yogurtchu YK. Solid State Commun 1999;112:489–94.
[18] Hassan MA, Hogarth CA. J Mater Sci 1988;23:2500.
[19] Godmanis IT, Tyukhin AN, Hubner K. Phys Status Solid B 1983;116:279.
[20] Saito K, Ikushima AJ. Phys Rev B 2000;62:8584.
[21] Hirota S, Izumitani T. J Non-Cryst Solids 1978;29:109.
[22] Betes T. In: Mackenzie JD, editor. Modern aspects of the vitreous state, vol. 2. London: Butterworths; 1962. p. 195.
[23] Canioni T, Segonds P, Srger L, Adamietz F, Ducasse A. Nucl Instr Meth 1995;B97:169.
[24] Vogel EM, Weber MJ, Krol DM. Phys Chem Glasses 1991;32:231.
[25] Cardinal T, Fargin E, Le Flem G, Canioni L, Segonds P, Srger L, et al. Eur J Solid State Inorg Chem 1994;31:935.
[26] Cardinal T, Fargin E, Nazabal V, Le Flem G, Le Boiteux S, Ducasse A. J Non-Cryst Solids 1998;239:131.
[27] Dimitrov V, Komatsu T. J Non-Cryst Solids 1999;249:160.
[28] Dimitrov V, Komatsu T. J Solid State Chem 2005;178:831.
[29] Boiteux Le, Segonds P, Canioni L, Srger L, Cardinal T, Duchesne C, et al. J Appl Phys 1997;81:1481.
[30] Hashimoto T, Uchida H, Takagi I, Nasu H, Kamiya K. J Non-Cryst Solids 1999;253:30.
[31] Zhu X, Meng Z. J Appl Phys 1994;75:3756.
[32] Zhu X, Li Q, Ming N, Meng Z. J Appl Phys Lett 1997;71:867.
[33] Shimoji N, Hashimoto T, Nasu H, Kamiya K. J Non-Cryst Solids 2003;324:50.
[34] Tan CZ, Arndt J. J Non-Cryst Solids 1997;222:391.
[35] Yano K, Morimoto Y. J Non-Cryst Solids 2004;349:120.
[36] Vogel EM, Kosinski SG, Krol DM, Jackel JL, Friberg SR, Oliver MK, et al. J Non-Cryst Solids 1989;107:244.
[37] Xiang Q, Zhou Y, Lam YL, Chan YC, Kam CH, Ooi BS, et al. Mater Res Bull 2000;35:1571.
[38] Martinet C, Paillard V, Gagnaire A, Joseph J. J Non-Cryst Solids 1997;216:77.
[39] Nazabal V, Fargin E, Ferreira B, Le Flem G, Desbat B, Buffeteau T, et al. J Non-Cryst Solids 2001;290:73.
[40] El-Alaily NA, Mohamed RM. Mater Sci Eng 2003;B98:193.
[41] Hauch A, Georg A, Baumgartner S, Krasovec UO, Orel B. Electrochim Acta 2001;46:2131.
[42] Heusing S, Sun D-L, Otero-Anaya J, Aegerter MA. Thin Solid Films 2006;502:240.
[43] Rao PN, Kanth CL, Rao DK, Veeraiah N, Quant J. Spectro Rad Transfer 2005;95:373.
[44] Villegas MA, Navarro JMF. J Euro Ceram Soc 2007;27:2715.
[45] Boye DM, Silversmith AJ, Nolen J, Rumney L, Shaye D, Smithb BC, et al. J Luminescence 2001;94–95:279.
[46] Toyohara N, Benino Y, Fujiwara T, Komatsu T. Solid State Commun 2006;140:299.
[47] Masai H, Tsuji S, Fujiwara T, Benino Y, Komatsu T. J Non-Cryst Solids 2007;353:2258.
[48] Raghavaiah BV, Laxmikanth C, Veeraiah N. Opt Commun 2004;235:341.
[49] Rao RB, Rao DK, Veeraiah N. Mater Chem Phys 2004;87:357.
[50] Kosaka S, Benino Y, Fujiwara T, Dimitrov V, Komatsu T. J Solid State Chem 2005;178:2067.
[51] Westin G, Ekstrand A, Zangellini E, Borjesson L. J Phys Chem Solids 2000;61:67.
[52] Vithal M, Nachimuthu P, Banu T, Jagannathan R. J Appl Phys 1997;81:7922.
[53] Karlsson KH, Liu G. J Non-Cryst Solids 2004;345&346:297.
[54] Su F, Deng Z. Opt Mater 2007;29:1452.
[55] Takahashi Y, Saitoh K, Benino Y, Fujiwara T, Komatsu T. J Non-Cryst Solids 2004;345& 346:412.
[56] Feitosa CAC, Mastelaro VR, Zanatta AR, Hernandes AC, Zanotto ED. Opt Mater 2006;28:935.
[57] Abdel-Baki M, Abdel Wahab FA, El-Diasty F. Mater Chem Phys 2006;96:201.
[58] Abdel-Baki M, El-Diasty F, Abdel Wahab FA. Opt Commun 2006;261:65.
[59] Astilean S, Lalanne P, Chavel P, Cambril E, Launois H. Opt Lett 1998;23:552.
[60] Sharonov MYu, Bykov AB, Owen S, Petricevic V, Alfano RR, Beall GH, et al. JOSA B 2004;21:2046.
[61] Mahnke M, Wiechmann S, Heider HJ, Blume O, Müller J. Int J Electron Commun 2001;55:342.
[62] Ravikumar RN, Komatsu R, Ikeda Ko, Chandrasekhar AV, Reddy BJ, Reddy YP, et al. Solid State Commun 2003;126:251.
[63] Mierczyk Z, Kwasny M, Kopczynski K, Gietka A, LÇ ukasiewicz T, Frukacz Z, et al. J Alloys Comp 2000;300–301:398.
[64] El-Hadi ZA. J Solid State Chem 2002;163:351.
[65] Munin E, Villaverde AB, Bass M, Richardson KC. J Phys Chem Solids 1997;58:51.
[66] Yanez-Limon JM, Perez-Roblez JF, Gonzalez-Hernandez J, Zamorano-Ulloa R, Ramirez-Rosales D. Thin Solid Films 2000;373:184.
[67] Grinberg M. Opt Mater 2002;19:37.
[68] Tanaka K, Tamura N, Hirao K, Soga N. Mater Chem Phys 1999;59:82.
[69] Felice V, Dussardier B, Jones JK, Monnom G, Ostrowsky DB. Opt Mater 2001;16:269.
[70] Jiang S, Myers M, Peyghambarian N. J Non-Cryst Solids 1998;239:143.
[71] Durga DK, Reddyb PY, Veeraiah N. J Luminescence 2002;99:53.
[72] Durga DK, Veeraiah N. Physica B 2002;324:127.
[73] Rao GV, Veeraiah N. J Alloys Comp 2002;339:54.
[74] Strek W, Deren PJ, Lukowiak E, Hanuza J, Drulis H, Bednarkiewicz A, et al. J Non-Cryst Solids 2001;288:56.
[75] El-Diasty F, Abdel-Baki M, Abdel Wahab FA, Darwish H. Appl Opt 2006;45:7818.
[76] El-Diasty F, Abdel Wahab FA, Abdel-Baki M. J Appl Phys 2006;100:093511.